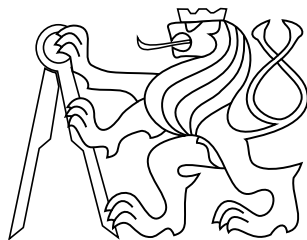


Bachelor's thesis

# **Detection and analysis of human eye pupil**

## **Detekce a analýza zornice lidského oka**

*Carin Koshel*



May 2015

Thesis advisor: Ing.Stanislav Vítek, Ph.D

Czech Technical University in Prague

Faculty of Electrical Engineering, Department of Radioelectronics

České vysoké učení technické v Praze  
Fakulta elektrotechnická

katedra radioelektroniky

## ZADÁNÍ BAKALÁŘSKÉ PRÁCE

Student: **Carin Koshel**

Studijní program: Komunikace, multimédia a elektronika  
Obor: Multimediální technika

Název tématu: **Detekce a analýza zornice lidského oka**

Pokyny pro vypracování:

1. Seznamte se s problematikou identifikace a analýzy vlastností zornice lidského oka ve videosekvenci
2. Implementujte vybrané algoritmy pro měření průměru zornice v programovém prostředí Matlab
3. Navrhněte vhodnou metodu předzpracování videosekvencí a diskutujte správnost a přesnost jednotlivých algoritmů

Seznam odborné literatury:

- [1] Mašek L., Recognition of Human Iris Patterns for Biometric Identification, Technical report, The University of Western Australia, 2003
- [2] Dušek, J., Jindra, T.: Measuring Biomechanics of the Vision Process, Sensory Fusion and Image Observation Features. In Technologies for Medical Sciences. London: Springer, 2012, p. 87-112. ISBN 978-94-007-4067-9.

Vedoucí: Ing. Stanislav Vítek, Ph.D.

Platnost zadání: do konce letního semestru 2015/2016

L.S.

doc. Mgr. Petr Páta, Ph.D.  
vedoucí katedry

prof. Ing. Pavel Ripka, CSc.  
děkan

V Praze dne 10. 2. 2015

## **Acknowledgement**

First of all, I would like to express my gratitude to my supervisor, Ing. Stanislav Vítek, Ph.D. for giving me the opportunity to work on this project. I appreciate his guidance and comments on my thesis and I would like to thank him for moral support.

I would like to acknowledge the help of my father, Koshel Uladzimir, who gave me his opinion on the thesis and provided me with helpful comments. Finally, I want to thank the whole my family for their love, encouragement and constant support through-out my studies.

## **Declaration**

I declare that I worked out the presented thesis independently and I quoted all used sources of information in accord with Methodical instructions about ethical principles for writing academic thesis.

## **Abstract**

Náplní této bakalářské práce je problematika rychlé detekce a analýzy zornice oka. Teoretický úvod práce je věnován popisu vybraných metod detekce zornice, dále možných metod předzpracování obrazu a jsou také shrnuty vlastnosti zornice, které budou použity pro komparativní analýzu.

Praktická část práce je zaměřena na experimenty s algoritmy implementovanými v programovém prostředí Matlab. Pro experimenty byly použity testovací videosekvence obsahující obraz lidských očí osvětlených infračerveným zdrojem světla.

## **Klíčová slova**

detekce duhovky a zornice; automatická segmentace; Houghova transformace; Daugmanův algoritmus; Starburst; Matlab

## **Abstract**

The bachelor's thesis introduces the problems of rapid detection and analysis of the parameters of the eye pupils. The theoretical part of the thesis provides description of selected pupil detection methods, as well as possible techniques of image preprocessing. In addition, the theoretical part provides a brief of pupil properties which will be used for the comparative analysis. The practical part is devoted to the experiments with algorithms implemented in Matlab environment. Video sequences of human eyes in the infrared lights were used as the test materials.

## **Keywords**

iris and pupil recognition; automatic segmentation; Hough transformation; Daugman algorithm; Starburst; Matlab

# Contents

<b>1</b>	<b>Introduction</b>	<b>1</b>
1.1	Motivation . . . . .	1
1.2	Problem statement . . . . .	2
1.3	Thesis structure . . . . .	3
<b>2</b>	<b>Analysis of issue</b>	<b>5</b>
2.1	General Eye Structure . . . . .	5
2.1.1	Eye's structure [3] . . . . .	5
2.1.2	Pupil and its functions . . . . .	7
2.2	Adaptation and Purkinje phenomenon . . . . .	7
2.2.1	Visual Adaptation . . . . .	7
2.2.2	Purkinje shift . . . . .	7
2.2.3	Purkynje images . . . . .	8
	Brightness of Purkinje images . . . . .	9
2.3	Eye measurements . . . . .	9
2.3.1	Types of eye movement . . . . .	9
	Saccadic movements . . . . .	9
	Smooth pursuit movements . . . . .	10
	Vergence . . . . .	10
	Vestibular Movements . . . . .	11
	The optokinetic reflex . . . . .	11
	Nystagmus . . . . .	12
2.3.2	Pupillary measurement: pupillometry and infrared videography .	12
	Techniques . . . . .	12
	Measurement's application . . . . .	13
<b>3</b>	<b>Preprocessing methods overview</b>	<b>14</b>
3.1	Edge Detection comparison . . . . .	14
3.1.1	Introduction . . . . .	14
3.1.2	Edge detection steps . . . . .	14
3.1.3	Edge detection classification . . . . .	14
	Sobel . . . . .	15

	Prewitt . . . . .	15
	Roberts . . . . .	15
	Laplacian of Gaussian (LoG) . . . . .	15
	Canny edge detector . . . . .	16
3.2	Filtration . . . . .	17
3.2.1	Gaussian filter [26] . . . . .	17
	How It Works . . . . .	17
	Features of Gaussian filter . . . . .	17
	Filter realization in Matlab . . . . .	18
3.2.2	Gabor filter . . . . .	18
	Gabor Annulus for Circle Detection . . . . .	19
<b>4</b>	<b>Algorithms' literature review</b>	<b>20</b>
4.1	Daugman's method . . . . .	20
4.2	Hough transformation . . . . .	21
4.2.1	Basic algorithm . . . . .	21
	Method challenges . . . . .	21
	Circular Hough transform . . . . .	22
4.2.2	Starburst . . . . .	23
<b>5</b>	<b>Experiments</b>	<b>24</b>
5.1	Analysis of algorithms . . . . .	24
5.1.1	Important distinctive features of algorithms . . . . .	25
	Daugman algorithm . . . . .	25
	Hough transformation . . . . .	26
	Starburst . . . . .	26
5.1.2	Test results of pupil center detection algorithms . . . . .	27
5.1.3	Execution time test . . . . .	27
5.1.4	Conclusion . . . . .	28
5.2	Preprocessing methods . . . . .	28
5.2.1	Image processing GUI . . . . .	29
5.2.2	Edge detectors comparison . . . . .	30
	Methodology [40] . . . . .	30

5.3	Daugman algorithm's improvement proposals . . . . .	31
5.3.1	Reduction of processing area . . . . .	31
5.3.2	Improvements based on the usage of the data obtained from the previous frame . . . . .	32
5.3.3	Improvements based on the preliminary image preparation . . .	32
5.3.4	Adaboost technique . . . . .	34
<b>6</b>	<b>Conclusion</b>	<b>35</b>
<b>Appendices</b>		
<b>A</b>	<b>The results of tests</b>	<b>37</b>
A.1	Algorithms comparison . . . . .	37
A.2	Edge detectors comparison table . . . . .	37
A.3	MSE diagram . . . . .	37
A.4	PSNR diagram . . . . .	38
<b>B</b>	<b>UserGuide of GUI Image_processing</b>	<b>39</b>
<b>C</b>	<b>CD content</b>	<b>41</b>
	<b>Bibliography</b>	<b>42</b>



# List of Figures

1	Sample image used in measurement of refractive conditions of a human visual system . . . . .	2
2	Eye's structure. Image taken from [4] . . . . .	5
3	The optical system of the eye. Image taken from [5] . . . . .	6
4	Red flower in the daylight and in the dim . . . . .	8
5	Purkunjé images. Image taken from [13] . . . . .	9
6	Convergence and divergence. Redrawn from [15] . . . . .	11
7	Nystagmus. Redrawn from [19] . . . . .	12
8	Gaussian curve with a 2-dimensional domain. Image taken from [5] . . . . .	17
9	Illustration of the iris boundary segmentation method based on the integro-differential operator. Image taken from [32] . . . . .	20
10	Example of <i>imfindcircles</i> application. Images are taken from [34] . . . . .	23
11	Image representation with the function <i>mesh</i> . . . . .	25
12	Zoom of the Gabor filter representation . . . . .	25
13	Example of <i>imcomplement</i> application . . . . .	26
14	Hough transformation application . . . . .	26
15	a) good and b) bad accuracy of Starburst . . . . .	27
16	Interface of <i>Image_processing</i> program . . . . .	29
17	Diagram of MSE results . . . . .	31
18	Diagram of PSNR results . . . . .	31
19	Example of <i>histeq</i> application . . . . .	32
20	Proposed algorithm: a) original image, b) detected edges, c) extension of white pixels, d) the previous image after <i>erosion</i> . . . . .	33
21	Adaboost result. Image taken from [41] . . . . .	34
22	Daugman algorithm was applied on figure 21. Image taken from [41] . . . . .	34



# 1 Introduction

## 1.1 Motivation

The objective of automatically search of the iris boundaries on the image occurs primarily at the early stages of processing input images in security systems and medical diagnostics.

The technique of identification using iris is widespread primarily due to its accuracy. Iris image is largely random, and the more randomness is, the greater the likelihood that a particular image is unique. Mathematically the <randomness> is described with the degree of freedom. The studies have shown that the texture of the iris has the freedom degree equal to 250, which is much greater than the degree of freedom of the fingerprint (35) and face images (20)[1]. In addition, unlike other biometric access control systems the identification with the iris image allows performing completely non-contact implementation.

Among ways of using this technology in the medical field there is the use for information on the state of the nervous system and other organs, as well as in psychiatric practice. Particular importance of assessing the state of the pupils is given in the diagnosis of a variety of neurological diseases. Such a direction as affective computing can be attributed to the field of psychology.

In addition to the abovementioned areas, the study of eye parameters is involved in a number of other disciplines, such as [2] cognitive sciences, human-machine interaction, marketing researches, perception of advertising, and in assistive technologies.

The eye tracking system has been used in communications equipment for fully paralyzed people since 2005. They allow typing text messages, sending emails, working on-line using only their eyes. Eye tracking allow achieving positive results even in the case of cerebral palsy in which the patient commits involuntary movements.

## 1.2 Problem statement

As mentioned above, the scope of eye image analysis is primarily information security and medicine. The large error can lead to incorrect identification or misdiagnosis. Therefore, it is necessary to reduce the likelihood of errors to a minimum. At the same time, most systems require real-time work and therefore ask for analysis algorithms fast enough. As an example of application where it is necessary to determine pupil features with high precision is a measurement of the refractive conditions of a human visual system, so-called accommodation and vergence. This measurement requires relatively complex calibration due to variable flux entering the eye and changing pupil diameter. Real-time evaluation of the pupil diameter would allow to establish a feedback and maintain a constant pupil diameter by change of the scene illumination.



**Figure 1** Sample image used in measurement of refractive conditions of a human visual system

Ideally, the result of the work is as follows: the absolutely identified pupil and its parameters at small time-consuming. However in reality, the situation is somewhat different. The task of achieving absolute accuracy is complicated by the following factors:

- Eyelashes, eyelids covering a certain area in the image
- Pupil defects
- Hotspots in the image
- Cosmetic lenses
- Head movements, blinking, inaccurate head positioning during image registration.

The abovementioned problems add the complexity to techniques, require a set of operations and as a result the work takes a lot of time. With the development of technologies there are opportunities for more efficient techniques that allow approaching closer to the ideal result. In this thesis, the following algorithms were reviewed and implemented:

- Daugman method
- Daugman method using Gabor filter
- Starburst
- Hough transformation

To optimize we chose Daugman algorithm as the most common. The main objective was to find such a solution in which the algorithm would work faster at maximum accuracy. Attempts for improving were made in two areas:

- **modification of the algorithm.** The difference between the two neighbouring images of video sequence is minimal, except in cases of eye movement (blinking). On this basis, the hypothesis of the possibility of accelerating the algorithm through data obtained from the previous image was put forward and verified. Another suggestion supposes reduction of the processed area of the image.

- **preprocessing of the images followed by the application of the original algorithm.** It should be understood that the processing itself takes a certain quantity of time, which is taken into account in assessing the speed of the algorithm. In my thesis in this area I have tested such preprocessing techniques as edges detectors, various filters, and morphological operations for the appropriateness of their use in work with eye imaging. Description of experiments along with the results is presented in the relevant chapter. At the end of the thesis there is a synthesis of the results of all the experiments and proposals for further work.

## 1.3 Thesis structure

The bachelor thesis can be presented structurally as follows:

Chapter 1. Introduction.

Chapter 2 is a brief analysis of the anatomical and physiological aspects of detection and includes the following subchapters:

- 2.1. General eye structure
- 2.2. Adaptation and Purkinje phenomenon.
- 2.3. Eye measurements

Chapter 3 includes a comparative overview of methods of image preprocessing used to improve the accuracy and speed of detection algorithms.

Chapter 4 provides a theoretical understanding of existing eye search techniques on the image, which later will be implemented practically and analyzed in Chapter 5.

## *1 Introduction*

Chapter 5 is devoted to the experiments' description.

Chapter 6 is the summary of what has been performed and accomplished.

## 2 Analysis of issue

### 2.1 General Eye Structure

#### 2.1.1 Eye's structure [3]

In the evolution eyes were formed as organs of sight providing the body with distant orientation in the optically heterogeneous environment. By their structure and mode of functioning it is a unique device converting light into the activity of the nervous tissue that underlies a variety of psychic phenomena: visual sensations, perceptions, ideas, and etc. The appearance of the human eye is shown in figure 2.

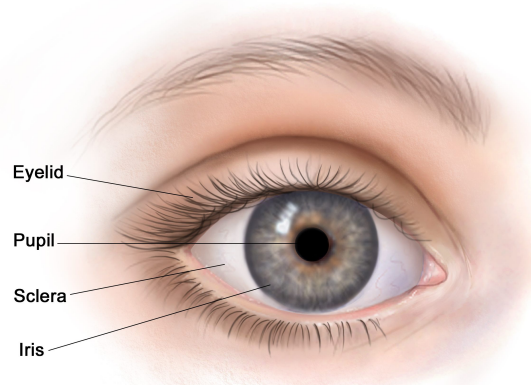


**Figure 2** Eye's structure. Image taken from [4]

Conjunctiva is a white connective tissue filled with small blood vessels, in the front of the eyeball becomes more curved and transparent cornea. Behind the cornea there is a pigmented (grey, blue or brown) iris framing the pupil. Depending on the light intensity the pupil diameter can vary. The conjunctiva and cornea are covered with a thin film of lacrimal fluid, which is distributed uniformly in eyelid moving (blinking). Lacrimal fluid improves the optical properties of the corneal surface, acts as a lubricant and protects the eye from infection penetration.

The optical system of the eye is not an accurately centred lens system which forms an inverted greatly reduced and distorted image (retinal image) of light sources. Reflected

## 2 Analysis of issue

light enters the eye through the cornea, passes through the crystalline lens having the ability to change its refractive power, the vitreous body (jelly-like fluid that fills the eye), a complex network of blood vessels, dendrites and axons of neurons, getting finally on the photosensitive surface of the retina.

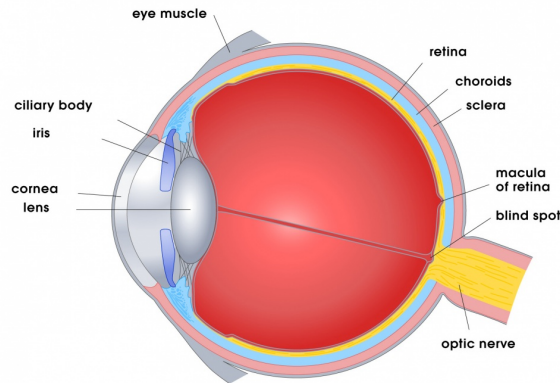


**Figure 3** The optical system of the eye. Image taken from [5]

Photosensitive cells (receptors) are distributed unevenly over the surface of the retina. They are concentrated the most densely in a small area near the intersection of the retina with the optical axis of the eye. This area – *fovea centralis* – provides the highest resolution of the eye. With increasing eccentricity the receptor density decreases gradually, and the resolution of the eye decreases. The exception is a small area of occurrence of the optic nerve in the eyeball - blind spot ( $16 - 18^\circ$  horizontal meridian of a nasal part of the retina). It is devoid of photoreceptors and is unable to cause the visual process. The retina of each eye enables perception of achromatic objects in the zone of  $150^\circ$  (horizontally) and  $130^\circ$  (vertically), wherein the centre of the field of view is shifted to the nasal part by approximately  $15^\circ$ .

Another property – mobility, or change in the location of the eyes in the orbit is closely related to heterogeneity of resolution. Eye is not only a vision organ, but also a movement organ. Every visual act involves oculomotor activity by which the search for a desired object is performed, its detection from the background, viewing, or “mental transformation”. This fact allows using eye movement parameters as indicators of the perceptual process and activity forms associated with it.



### 2.1.2 Pupil and its functions

The pupil of the human eye is a hole in the iris. The aim of the pupil is to control the light entering the retina. The pupil size varies depending on how light irritates it, whether eyes are crossed, whether they are strained or relaxed. In other words, the size of the pupil can say a lot about their state. Consequently, the attention should be given to the size of the pupils in diagnosing any problems with the vision, as well as in examining some diseases of the internal organs and systems.

Normally, the pupil diameter varies from 3 to 8 mm [6], physiological anisocoria is allowed up to 0.8 mm. The increased activity of the sympathetic innervation causes dilation of the pupils, while their constriction indicates an increase in the activity of the parasympathetic innervation. The pupil is never absolutely calm. Its constant movements depend on many external and internal stimuli. Moderate daylight, a state of an increased activity, emotional stress, and fear cause dilation of the pupil. During sleep or resting state, depression or fatigue pupils are constricted. It can be assumed that the eye reflects to some extent the energy and emotional human potential: wide pupils indicate a high level of the potential, narrow pupils – low one.

## 2.2 Adaptation and Purkinje phenomenon

### 2.2.1 Visual Adaptation

The eye adapts to changing light level, altering light sensitivity like a camera modifies exposure[7]. Adaptation is an essential, but frequently overlooked issue in many instances. A person's perceptual ability is determined, not only by the scene viewed at the time of the accident, but also by what he had previously viewed.

There are four types of adaptation. The eye can dark adapt, going from bright to dark environment, and vice versa. For each one of them, exist two variations, a slow and a transient phase.

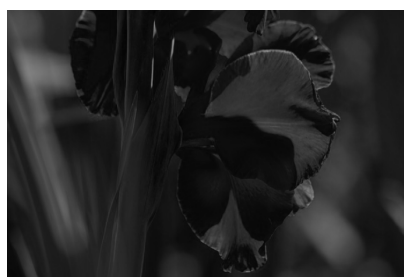
### 2.2.2 Purkinje shift

The Purkinje effect is the reduction in the luminosity of a red light relative to that of a blue light when the luminances are reduced from photopic to scotopic levels of illumination [8].

## 2 Analysis of issue

The causes of this are found in the retina's outer nuclear layer structure, which contains two types of cells, cone cells and rod cells. The rods are more multitudinous than the cones. They work under low light conditions and provide scotopic vision. The cones are dominant in well-lit conditions and in charge of the color discrimination. There are normally three types of cone cell, but overall they are most sensitive to yellow light.

Thereby, in the daylight, red flowers (which contain a lot of yellow) seem to be very bright, as seen by the cones in the retina. Under very low levels of light, the rods which are most sensitive to blue/green wavelengths, see the surrounding leaves as being brighter than the red flower [9].



a) well-lit conditions (taken from [10])    b) low light conditions (created using [11])

**Figure 4** Red flower in the daylight and in the dim

### 2.2.3 Purkynje images

Purkinje images (also Purkinje reflexes, Purkinje-Sanson images [12] [13]) are reflections of objects from the structure of the eye. Typically, not less than four Purkinje images are visible. The first of these arises on the interface between the air and the outer surface of the cornea and it is bright and erect. Owing to the great difference in refraction indices, it has the greatest intensity. The second Purkinje image is the reflection from the inner surface of the cornea. The third Purkinje image is the reflection from the anterior surface of the lens. The intensity of this image is very low. The fourth Purkinje image is the reflection from the posterior surface of the lens. The fourth image as distinct from others is an inverted image.

The first and fourth Purkinje images are used by some eye trackers, devices to measure the position of an eye. The cornea reflection (the first image) used in this measurement was given a name *glint*.

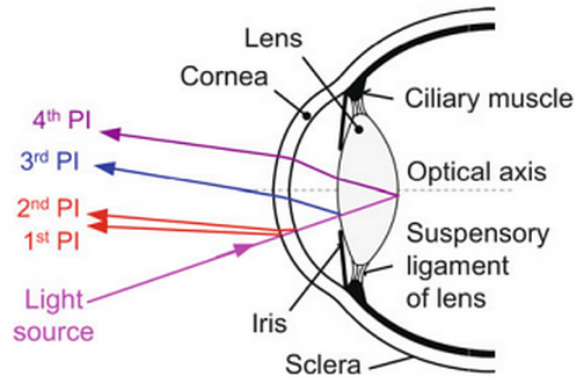


**Figure 5** Purkinje images. Image taken from [13]

### Brightness of Purkinje images

The brightness of the Purkinje images can be determined using *Fresnel's equation*:

$$Brightness = \left( \frac{n' - n}{n' + n} \right)^2, \quad (1)$$

where  $n$  and  $n'$  are the refractive indices before and after the reflecting surface. As was already stated above, the first Purkinje image is the brightest of the four. The Purkinje images can be used to assess the curvatures and separations of the surfaces in the eye.

## 2.3 Eye measurements

### 2.3.1 Types of eye movement

For any application of eye movement instrumentation, the kinds of eye movements to be observed must be clearly understood so that the instrument specifications may be assigned properly. The following subchapter summarizes the types of known eye movements. There are six different types of eye movement. Each type of movement serves a different function in visual perception [14].

#### Saccadic movements

Saccadic movements are very rapid, ballistic movements that bring new objects of interest into the fovea. Saccades are said to be ballistic because once it starts, it will not stop until it reaches the target location. Saccades are also very quick. A single saccade only takes about 150-200 ms to plan and execute. The act of movement is also very fast, the velocity can achieve  $900^\circ/\text{s}$  degrees per second. The quick movements

allow the eyes to concentrate on various parts of the visual world to gather information and paint a grand picture in our brains.

### Smooth pursuit movements

Smooth pursuit movements are used to track moving objects. This is an important function because most objects move. Without the ability to track moving objects, we would not even be able to walk safely on the streets because we won't be able to perceive cars, bikes, etc. There are four primary differences between smooth pursuit movements and saccades:

- **manner of movement.** Smooth pursuit movements are smooth and continuous, but saccades move in a jerky and abrupt way.
- for smooth pursuit movements a **feedback is constantly required** to track the moving object.
- **speed difference.** Smooth pursuit movements can move at 100 degrees per second whereas saccades' possible velocity is 900 degrees per second.
- **distinct amount of clarity.** The tracked object is clear, however, everything in the environment which does not move at the same direction or speed would appear smeared. The speed of the moving object determines how well we can track the object. The faster it moves, the harder it is for our eyes to catch up. People are born with an innate ability to track object; however, through practice, the ability could be improved.

### Vergence

Vergence eye movements are movements of the two eyes in opposite directions in order to fuse the image of near or far objects. Vergence movements are very slow compared to other eye movements with the velocity about  $10^\circ/\text{s}$ .

Vergence movement's purpose is to select the distance of the object we want to observe. Saccades and smooth pursuit movements help us focus the object at the fovea, but without vergence movement, the eyes will not converge to the point of interest. Our eyes will converge less for farther objects and converge more for closer objects. If you look from a far object to a near one, vergence eye movements are generated. Looking from far to near is convergence and looking from near to far is divergence.

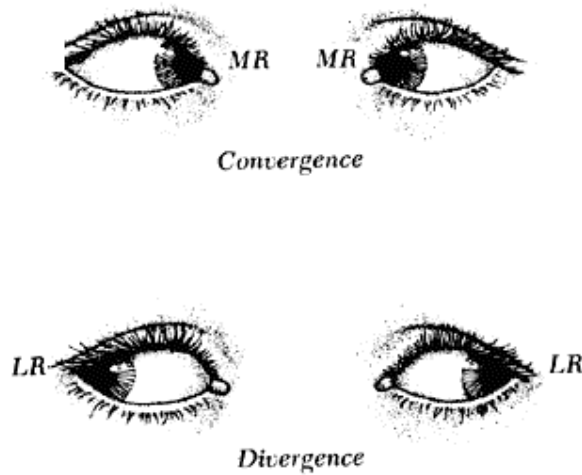


**Figure 6** Convergence and divergence. Redrawn from [15]

Vergence movements are closely connected to accommodation of the eye. Under normal conditions, changing the focus of the eyes to look at an object at a different distance will automatically cause vergence and accommodation, sometimes known as *the accommodation-convergence reflex* [16].

### **Vestibular Movements**

Vestibular cooperates with optokinetic movements to preserve the image on the center of the visual field during head movements. This movement will move the eyes in the opposite direction of the head to keep the eyes focused on the same point at all times. The vestibular system in the inner ear directs vestibular movements by providing information about changing of the head position and orientation. When the head moves, the vestibular apparatus would send signals to the eyes to compensate for the movements. Although vestibular movements are more sluggish than saccades, they are swifter and more accurate than smooth pursuit movements, moreover, *vestibulo-ocular reflex* is one of the fastest reflexes in the human body [17].

### **The optokinetic reflex**

The optokinetic reflex is a combination of a saccade and smooth pursuit eye movements. It is seen when an individual follows a moving object with their eyes, which then moves out of the field of vision at which point their eye moves back to the position it was in when it first saw the object. The reflex develops at about 6 months of age [18].

## Nystagmus

Nystagmus is a condition of involuntary (or voluntary, in rare cases) eye movement, acquired in infancy or later in life, that may result in reduced or limited vision. Function of nystagmus is disorders' compensation of the visual and vestibular systems or maintain the efficiency of the perception of the moving elements of the environment, which has a regular structure [3].



**Figure 7** Nystagmus. Redrawn from [19]

There are two key forms of nystagmus: pathological and physiological, with variations within each type. Nystagmus may be caused by congenital disorders, acquired or central nervous system disorders, toxicity, pharmaceutical drugs, alcohol, or rotational movement. Previously considered untreatable, in recent years several pharmaceutical drugs have been identified for treatment of nystagmus. Nystagmus is occasionally associated with vertigo [18].

### 2.3.2 Pupillary measurement: pupillometry and infrared videography

#### Techniques

Pupillary measurement methods [20] have varied from direct observation using rulers or circles, photographic techniques, and electronic pupillographs to computerized pupillometry.

At the present time the pupil size and movement are measured mostly by either infrared videography or computerized pupillometry.

Infrared videography is used in order to detect a magnified movement of both pupils at the same time. The technique allows the pupils to be visualized in the dark, and therefore is used to confirm difficult-to-test afferent pupillary defects. Such cases may occur when an iris is heavily pigmented. Infrared videography takes the advantage of

such dark pigmentation, since melanin actually reflects the infrared light shone on to the iris. Therefore, pigmented irises appear light on the screen, and the black pupils stand out in contrast to the surrounding light-appearing iris.

In contrast to infrared videography, computerized pupillometry is able to record the pupil size and movement in the light as well as in dark. These instruments can record digitally, then analyze with sophisticated software algorithms various types of information gathered by the testing. Digital pupillometers enable to assess rapidly and accurately the pupil size.

### **Measurement's application**

Pupillometry has long been used in a research setting to study the autonomic nervous system, pain responses, psychology, fatigue and sleep disorders [20]. A rapid development of the technology allows using computerized pupillometry in the clinical realm. Dynamic, perfectly exact measurement of the pupil size finds broad application in several medical and ophthalmic sub-specialties tests.

Measuring the pupil size is particularly useful for refractive surgeons because large pupils measured preoperatively correlate with increased post-LASIK visual disturbances during scotopic conditions. Neuro-ophthalmologists are interested in pupillometry to distinguish physiological anisocoria from Horner syndrome, for the determination of lesions of the afferent (retina, optic nerve) and efferent pathways, and even plot visual fields through measuring graded pupil constriction to focal light stimuli. Other medical specialties also use clinical pupillometers for diagnosis.

## 3 Preprocessing methods overview

### 3.1 Edge Detection comparison

#### 3.1.1 Introduction

Edge detection is the name for a set of mathematical methods which aim at identifying points in a digital image at which the image brightness has discontinuities. The points at which image brightness changes sharply are typically organized into a set of curved line segments termed *edges* [21].

The main objective of this subchapter is to make a theoretical review and to compare existing techniques for ability of their application in pupil detection.

#### 3.1.2 Edge detection steps

Edge detection process including the following steps [22]:

- **Smoothing.** Suppressing noise as much possible, without destroying the true edges;
- **Enhancement.** Apply a filter to enhance the quality of the edges in the image (sharpening);
- **Detection.** Decisive about which edge pixels should be superfluous as noise and which should be retained;
- **Localization.** Determine the accurate locations of an edge. Edge thinning and linking are generally a requisite for edge localization.

#### 3.1.3 Edge detection classification

The edge detection algorithms can be generally classified based on the behavioural study of edges with respect to the operators. Different edge-detection approaches can be broadly classified under Classical or Gradient based edge detectors (first order derivative), Zero crossing (second order derivative) and Optimal edge detector [23].



**Sobel**

The Sobel edge detector computes the gradient by using the discrete differences between rows and columns of a  $3 \times 3$  neighborhood. The Sobel operator is based on convolving the image with a small, separable, and integer valued filter:

$$G_x = \begin{pmatrix} -1 & 0 & 1 \\ -2 & 0 & 2 \\ -1 & 0 & 1 \end{pmatrix}, G_y = \begin{pmatrix} 1 & 2 & 1 \\ 0 & 0 & 0 \\ -1 & -2 & -1 \end{pmatrix}$$

**Prewitt**

Prewitt operator is the one of the oldest and best understood methods of detecting edges in images. The Prewitt edge detector uses the following mask to approximate digitally the first derivatives  $G_x$  and  $G_y$ :

$$G_x = \begin{pmatrix} -1 & -1 & -1 \\ 0 & 0 & 0 \\ 1 & 1 & 1 \end{pmatrix}, G_y = \begin{pmatrix} -1 & 0 & 1 \\ -1 & 0 & 1 \\ -1 & 0 & 1 \end{pmatrix}$$

**Roberts**

In Roberts edge detection, the vertical and horizontal edges bring out individually and then put together for resulting edge detection.

The Roberts operator is defined as:

$$G(x, y) = \left\{ \left[ \sqrt{f(x, y)} - \sqrt{f(x+1, y+1)} \right]^2 + \left[ \sqrt{f(x+1, y)} - \sqrt{f(x, y+1)} \right]^2 \right\}^{1/2} \quad (2)$$

and uses the following masks to approximate digitally the first derivatives as differences between adjacent pixels:

$$G_x = \begin{pmatrix} 1 & 0 \\ 0 & -1 \end{pmatrix}, G_y = \begin{pmatrix} 0 & 1 \\ -1 & 0 \end{pmatrix}$$

**Laplacian of Gaussian (LoG)**

This detector finds edges by looking for zero crossings after filtering  $f(x, y)$  with a Laplacian of Gaussian filter. In this method, the Gaussian filtering is combined with Laplacian to break down the image where the intensity varies to detect the edges effectively. It finds the correct place of edges and testing wider area around the pixel. There

are different ways to find an approximate discrete convolution kernel that approximates the effect of the Laplacian. A possible kernel is

$$\begin{pmatrix} 0 & -1 & 0 \\ -1 & 4 & -1 \\ 0 & -1 & 0 \end{pmatrix},$$

which is a positive Laplacian because the central peak is positive.

The 2-D LoG function centered on zero and with Gaussian standard deviation  $\sigma$  has the form:

$$LoG(x, y) = -\frac{1}{\pi\sigma^4} \left[ 1 - \frac{x^2 + y^2}{2\sigma^2} \right] e^{-\frac{x^2 + y^2}{2\sigma^2}} \quad (3)$$

#### Canny edge detector

Based upon Marr and Hildreth algorithm, Canny edge detector is supposed to be an optimal edge detection technique as provide good detection, clear response and good localization. It is probably the most widely used detector in the sphere of image processing.

The algorithm runs in 5 separate steps [24]:

- **Smoothing.** Blurring of the image to remove noise.
- **Finding gradients.** The edges should be marked where the gradients of the image has large magnitudes;
- **Non-maximum suppression.** Only local maxima should be marked as edges;
- **Double thresholding.** Potential edges are determined by thresholding;
- **Edge tracking by hysteresis.** Final edges are determined by suppressing all edges that are not connected to a very certain edge.

Since the Canny edge detector is sensitive to noise contained in the unprocessed source imagery, it uses a filter based on a Gaussian curve, where the raw image is convolved with a Gaussian filter. As a result, a slightly blurred version of the original is obtained, which is not affected by a single noisy pixel to any significant degree [25].

## 3.2 Filtration

### 3.2.1 Gaussian filter [26]

#### How It Works

The Gaussian distribution in 1-D has the form:

$$G(x) = \frac{1}{\sqrt{2\pi}\sigma} e^{-\frac{x^2}{2\sigma^2}}, \quad (4)$$

where  $\sigma$  is the standard deviation of the distribution. We have also assumed that the distribution has a mean of zero (i.e. it is centered on the line  $x = 0$ ). The distribution is illustrated in figure below

In 2-D, an isotropic (i.e. circularly symmetric) Gaussian has the form

$$G(x, y) = \frac{1}{2\pi\sigma^2} e^{-\frac{x^2+y^2}{2\sigma^2}} \quad (5)$$

This distribution is shown in Figure 8:

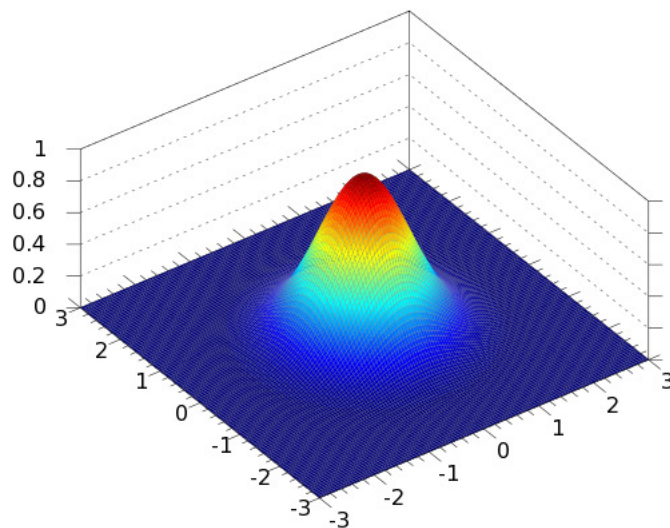


**Figure 8** Gaussian curve with a 2-dimensional domain. Image taken from [5]

#### Features of Gaussian filter

The following features are of interest in this type of filter:

- Remove “high-frequency” components from the image (low-pass filter);
- Convolution with self is another Gaussian;

### 3 Preprocessing methods overview

- So it can smooth with small-width kernel, repeat, and get same result as larger-width kernel would have.

- Convolution with two Gaussian kernels of width  $\sigma$  is same as convolution once with kernel of width  $\sqrt{2}\sigma$ .

• **Separable kernel.** The 2D Gaussian can be expressed as the product of two functions. One is a function of  $x$  and the other is a function of  $y$ . In this case, two functions are the 1D Gaussian.

$$G_{\sigma}(x, y) = \frac{1}{2\pi\sigma^2} \exp\left(-\frac{x^2+y^2}{2\sigma^2}\right) = \left(\frac{1}{\sqrt{2\pi}\sigma} \exp\left(-\frac{x^2}{2\sigma^2}\right)\right) \left(\frac{1}{\sqrt{2\pi}\sigma} \exp\left(-\frac{y^2}{2\sigma^2}\right)\right) \quad (6)$$

#### Filter realization in Matlab

Function  $h = fspecial('gaussian', hsize, sigma)$  [27] returns a rotationally symmetric Gaussian lowpass filter of size  $hsize$  with standard deviation  $sigma$ .  $Hsize$  can be a vector specifying the number of rows and columns in  $h$ , or it can be a scalar, in which case  $h$  is a square matrix. The default value for  $hsize$  is [3 3]; the default value for  $sigma$  is 0.5.

#### 3.2.2 Gabor filter

Gabor filters have many applications in biologically inspired systems, especially those related to computer vision, since their responses are similar to those of the nerves in the V1 region in the visual cortex [28]. Gabor functions act as low-level oriented edge and texture discriminators and are sensitive to different frequencies and scale information. These facts raised considerable interest and motivated researchers to explore extensively the properties of Gabor functions [29].

Mathematically, a 2D Gabor function is the product of a 2D Gaussian and a complex exponential function and can be defined as follows:

$$g_{\theta, \gamma, \sigma}(x, y) = \exp\left\{-\frac{x^2 + y^2}{2\sigma^2}\right\} \exp\left\{\frac{j\pi}{\gamma\sigma}(x \sin \theta - y \cos \theta)\right\} \quad (7)$$

The response of a Gabor filter to the image  $I(x, y)$  is obtained via a convolution operation. This response at point  $(x_0, y_0)$  is calculated as follows:

$$G_{\theta, \gamma, \sigma}(x_0, y_0) = (I * g_{\theta, \gamma, \sigma})(x_0, y_0) = \int I(x, y) g_{\theta, \gamma, \sigma}(x_0 - x, y_0 - y) dx dy \quad (8)$$

Thus, emphasis of different types of image characteristics is achieved by an appropriate choice of the  $\sigma, \theta, \gamma$  combination.

### Gabor Annulus for Circle Detection

A circular object detection method using Gabor ring is based on convolution filtration of the image using a modified Gabor wavelets. The core of the convolution filter is designed according to the formula [30]:

$$G(x,y) = \frac{1}{2\pi\sigma r_0} e^{-\pi[\frac{(x-r_0)^2}{\sigma^2}]} e^{i[2\pi f_0(r-r_0)]}, \quad (9)$$

where  $r$

$$r = \sqrt{(x-x_0)^2 + (y-y_0)^2}, \quad (10)$$

$\sigma$  denotes the standard deviation of the Gaussian envelope and  $r_0$  is the radius of the ring. The second exponent is a complex plane wave with the frequency  $f_0$  in the direction of the waveform.  $(x_0, y_0)$  indicates the coordinates of the center of the filter in the spatial domain.

## 4 Algorithms' literature review

### 4.1 Daugman's method

Daugman presented [31] the first approach to computational iris recognition, including iris localization. An integro-differential operator is proposed for locating inner and outer boundaries of an iris. The operator assumes that pupil and limbus are circular contours and performs as a circular edge detector. Detecting the upper and lower eyelids is also performed using the integro-differential operator by adjusting the contour search from circular to a designed accurate. Integro-differential operator is defined as:

$$\max(r, x_0, y_0) \left| G_\sigma(r) * \frac{\partial}{\partial r} \oint_{r, x_0, y_0} \frac{I(x, y)}{2\pi r} ds \right|, \quad (11)$$

where  $I(x, y)$  is input image of an eye. The integro-differential operator searches over the image domain  $(x, y)$  for the maximum in the blurred partial derivative with respect to increasing radius  $r$  of the normalized contour integral of  $I(x, y)$  along a circular arc  $ds$  of radius  $r$  and center coordinates  $(x_0, y_0)$ . The symbol  $*$  stands for convolution and  $G_\sigma(r)$  is a smoothing function such as a Gaussian of scale  $\sigma$  and is defined as:

$$G_\sigma(r) = \frac{1}{\sqrt{2\pi}\sigma} e^{-\frac{(r-r_0)^2}{2\sigma^2}} \quad (12)$$

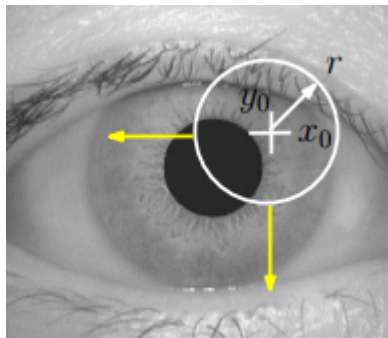


**Figure 9** Illustration of the iris boundary segmentation method based on the integro-differential operator. Image taken from [32]

## 4.2 Hough transformation

The Hough transform is a feature extraction technique used in image analysis, Computer Vision, and image processing. The purpose of this transform is to find imperfect case of objects of a certain class of shapes by a voting procedure. This voting procedure is performed in a parameter space from which the candidate objects are obtained as local maxima in a storage matrix which is constructed by the algorithm explicitly calculating the Hough transform. The original Hough transform only concerned the identification of lines in the image. Later, the generalized Hough transform was invented to extend the number of identified shapes, like circles or ellipses.

### 4.2.1 Basic algorithm

The basic algorithm of curves detection consists of the following steps [33]:

- 1) **Selection of the sampling grid.** At this stage we should choose a sampling interval for each curve parameter. The complexity ( $\sim$  rate) and the efficiency of the algorithm will depend on this choice;
- 2) **Filling accumulator (counters matrix).** Often, this is the longest step of the algorithm, since the filling is made by means of complete enumeration. The complexity of the algorithm depends on the first step and is  $O(N * M)$ , where  $N$  is a number of points,  $M$  is a number of cells of the accumulator;
- 3) **Analysis of the accumulator (peaks search).** The counter with the maximum value is searched in the accumulator matrix;
- 4) **Curve detection.** Each accumulator cell is a value of the phase space, which means that it defines a certain (desired) curve. Since the value in *step1* has become discrete, the clarification of the curve in any other method with already found points of the curve may be required;
- 5) **Subtract from the accumulator.** A temporary accumulator is calculated for the points of the detected curve and subtracted point-by-point from the main one;
- 6) **Go to step 3.**

### Method challenges

- **Sampling.**

The sampling grid was chosen as the step 1. The following challenges can occur in connection with this choice:

- The chosen grid is too small. Then, if noise was in the original point cloud, even points of one curve will get in different grid cells, and therefore, the potential maximum of the accumulator (corresponding to this curve) will be *fuzzy* and it will be difficult or impossible to find;
- The grid is chosen too large. Then there is the possibility that points lying on different curves will get in one cell.

- **The complexity of the algorithm.**

Filling the accumulator in step 2 is the most time consuming part of the algorithm, the complexity of which depends on: the dimension of the phase space and grid sampling. The larger  $\Phi$  dimension and the smaller grid are, the more cells in the accumulator are. So, the more memory and time for its storage and filling is necessary. That is why, in practice, more often the phase space is a subspace, and Hough transformation is used primarily to search for right lines in the subspace (images).

### Circular Hough transform

In a circular Hough transform, images are analyzed to estimate the three parameters of one circle,  $(x_0, y_0, r)$  using following equations [27]:

$$H(x_0, y_0, r) = \sum_i h(x_i, y_i, x_0, y_0, r), \quad (13)$$

where  $h$

$$h(x_i, y_i, x_0, y_0, r) = \begin{cases} 1, & \text{if } g(x_i, y_i, x_0, y_0, r) = 0 \\ 0, & \text{otherwise} \end{cases}, \quad (14)$$

$g$  is determined by the equation of the following pattern:

$$g(x_i, y_i, x_0, y_0, r) = (x_i - x_0)^2 + (y_i - y_0)^2 - r^2 \quad (15)$$

### Matlab function *imfindcircles*

Being Matlab implementation of circular Hough transform, the function *imfindcircles* is used to detect circumferences on the images. Here is illustrated which parameters are required in *imfindcircles* [34]:



```

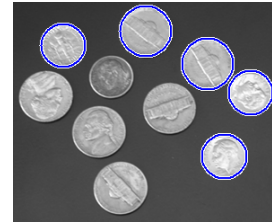
centers = imfindcircles(A,radius)
[centers,radii] = imfindcircles(A,radiusRange)
[centers,radii,metric] = imfindcircles(A,radiusRange)
[centers,radii,metric] = imfindcircles( __, Name,Value),

```

where  $A$  is an input image;  $radius$  is circle radius;  $radiusRange$  is range of radii respectively.



a) original image

b) after *imfindcircles*

**Figure 10** Example of *imfindcircles* application. Images are taken from [34]

#### 4.2.2 Starburst

Searching circular objects using Starburst method [35] combines likewise the gradient method both detection of possible edge points of the pupil and RANSAC method for calculating parameters of the optimal circle for the candidate points. The difference is in the method of determining the candidate points. Detection is based on the analysis of brightness profiles according to selected lines in the image. From a predetermined or randomly selected point a limited number of lines in the full angle range is kept. In the direction of the lines derivative is determined for each point and from the resulting function using thresholding possible points of the pupil-iris boundary are selected. Then from each obtained point back lines are drawn to the other points that are evaluated in the same way. Location gravity found points converge gradually toward the center of the pupil and the final group of candidate points is so limited by the amount of points lying outside desired edge. The acquired points are further processed with RANSAC method adapted for detecting circular objects.

## 5 Experiments

Experiments in this part of the thesis were conducted in three stages. At the initial stage a program for image preprocessing was written in the Matlab environment to allow visual demonstration of application of selected techniques. Then the comparative analysis of the edge detectors was made to identify which one is the best. In closing, attempts to improve Daugman algorithm application on tested images were undertaken.

### 5.1 Analysis of algorithms

In this part of the thesis the benchmark analysis of algorithms was made. As comparative aspects the execution time of each algorithm to 25 images, the average execution time of the algorithm, and the accuracy rate of center detection and radii were chosen[36][37]. The tests were conducted on the PC with the following system parameters:

Processor *Intel(R) Core(TM)2 CPU, 1.86 GHz*

RAM memory *4.0 GB*

System type *64-bit Operating System*

Employed source codes intended for operating with images of 2 eyes, but in medical practice the properties of each eye has to be analyzed separately, therefore some corrections were made for further work.

First of all, sequence of, so-called, ground truth images was created. These images are defined to be reference samples and obtained values should be compared with values, obtained from this sequence.

For creating a material for comparisons, global image threshold was chosen using Otsu's method, which is implemented in Matlab as a function *graythresh*. It was revealed, that the source code of Starburst algorithm, as well as the code of Hough transformation, are unable to work with this image type. In order to solve this problem, I processed the obtained images with some tools from Photoshop editor.

### 5.1.1 Important distinctive features of algorithms

Important distinctive features of algorithms are described briefly below. UserGuide on the enclosed CD has more details concerning how these programs work.

#### Daugman algorithm

Two versions of this algorithm with and without Gabor filter were tested and compared. Version with Gabor filter is realized by amending the basic Daugman algorithm code. Alterations are related to the *search* function. Henceforth, the center coordinates obtained by the Gabor filter are declared as an argument of search function. Also, bicubic interpolation appears in this variation for getting more precise result [36].

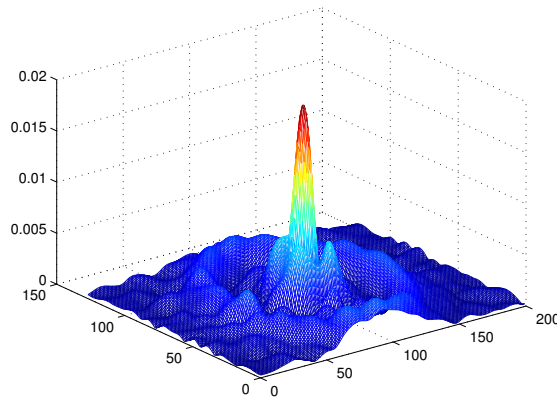
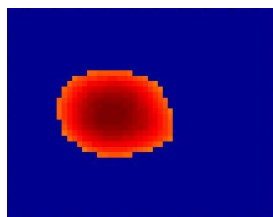
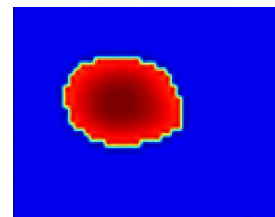


**Figure 11** Image representation with the function *mesh*



a) before bicubic interpolation



b) after bicubic interpolation

**Figure 12** Zoom of the Gabor filter representation

Summarizing the results, I came to a conclusion that adding of Gabor filter led to unjustifiable prolongation of the routine (2.08-fold time increase and only 1% of improvement)

### Hough transformation

Preliminarily, testing images have to be inverted, because the algorithm work only with dark pupil. There is a special function integrated in Matlab called *imcomplement* therefore [38].



**Figure 13** Example of *imcomplement* application

After *imcomplement* operation, algorithm was successfully launched.

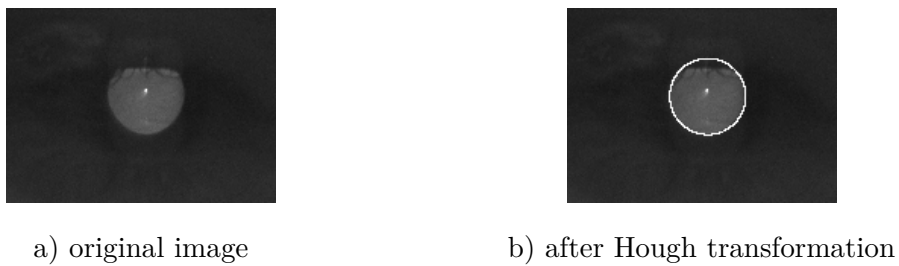


**Figure 14** Hough transformation application

### Starburst

Analogously to Hough algorithm, first of all images have to be inverted. It should also be mentioned that radius  $r$  and eccentricity  $e$  are not computed in this code, they can be calculated in the following way:

$$e = \sqrt{1 - \frac{b^2}{a^2}} \quad (16)$$

and

$$r = \frac{b}{\sqrt{1 - e^2 \cos^2 \varphi}} \quad (17)$$

Figures below demonstrate an example of good and bad Starburst result.



**Figure 15** a) good and b) bad accuracy of Starburst

### 5.1.2 Test results of pupil center detection algorithms

For each method of pupil center detection Euclidean distance was calculated from the formula 18.

$$l = \sqrt{(x_{gt} - x_e)^2 + (y_{gt} - y_e)^2}, \quad (18)$$

where  $l$  is the length between center points in pixels,  $(x_{gt}, y_{gt})$  are coordinates from ground truth image,  $(x_e, y_e)$  are coordinates obtained experimentally.

#### A particular example of calculations:

image\center coordinates	x-axis coordinate	y-axis coordinate
the ground truth image	58.764	92.748
the tested image	58.764	93.456

**Table 1** Sample data used in determining the accuracy of detecting the center of the pupil

$$l = \sqrt{(58.764 - 58.764)^2 + (92.748 - 93,456)^2} = \sqrt{0.501} = 0.708 \text{ [pixels]}$$

### 5.1.3 Execution time test

Time was noted with a *tictoc* function. Function's keywords were placed in manner that allows to know the time consumption without drawing plots.

Test results indicate that time consumption varies from time to time. There are numerous of possible explanations for this fact, eg. because right now the operating system executes other operation on the bus or on the disk, which slightly slows down the process. The abovementioned must be taken into account for achieving correct results and making a right conclusion, so all algorithms were launched 10 times and the average of values was calculated. These values are presented in the table 2

## 5 Experiments

algorithm	Daugman	Daugman with Gabor	Starburst	Hough transformation
algorithm's execution time for 25 images [s]	24.391	50.661	25.896	0.955
average algorithm's execution time [s]	0.976	2.026	1.036	0.038
accuracy [%]	98	99	78	97
average precision center [pixels]	0.721	0.649	5.616	0.9296

**Table 2** Experimental results

### 5.1.4 Conclusion

Based on the obtained data, it can be concluded that Daugman without Gabor filter is considered to be the optimum. In the next stages Hough transformation, Daugman with Gabor filter are ranked. The worst result was performed by Starburst algorithm - the last but one in the time consumption test and inferior accuracy (1.04 seconds per image with precision of 78%). Hough transformation yielded surprisingly good results, but I decided not to adopt it as the first-rate algorithm. Instead, I test it and Daugman algorithm on images from the other database. As a result, I came to a conclusion that Daugman method findings were better.

## 5.2 Preprocessing methods

Source data pretreatment is a very important component in the algorithm of pupil detection, exerting influence on the reliability and accuracy of the resulting data. Based on these considerations, it was concluded that this subject deserves special attention and should be studied in the experimental part of the thesis.

The essence of the image preprocessing is to enhance the quality of initial material. Numerous techniques can be used at the stage of preliminary image preparation such as filtering, morphological operators, histogram optimization. The optimum combination should be selected depending on the object being pursued, and also depending on the properties of the source data. In terms of segmentation, binarization and obtaining a contour image representation are among the most significant ones.

Experiments in this part of the thesis took place in three stages. The first step was to write a GUI program for image preprocessing. Then edge detectors were dissected

to find the best one. In the end I chose the algorithm to improve the image sequences presented on the enclosed CD.

### 5.2.1 Image processing GUI

This program is a tool for image processing. It was established in Matlab environment and has a user-friendly graphical interface.

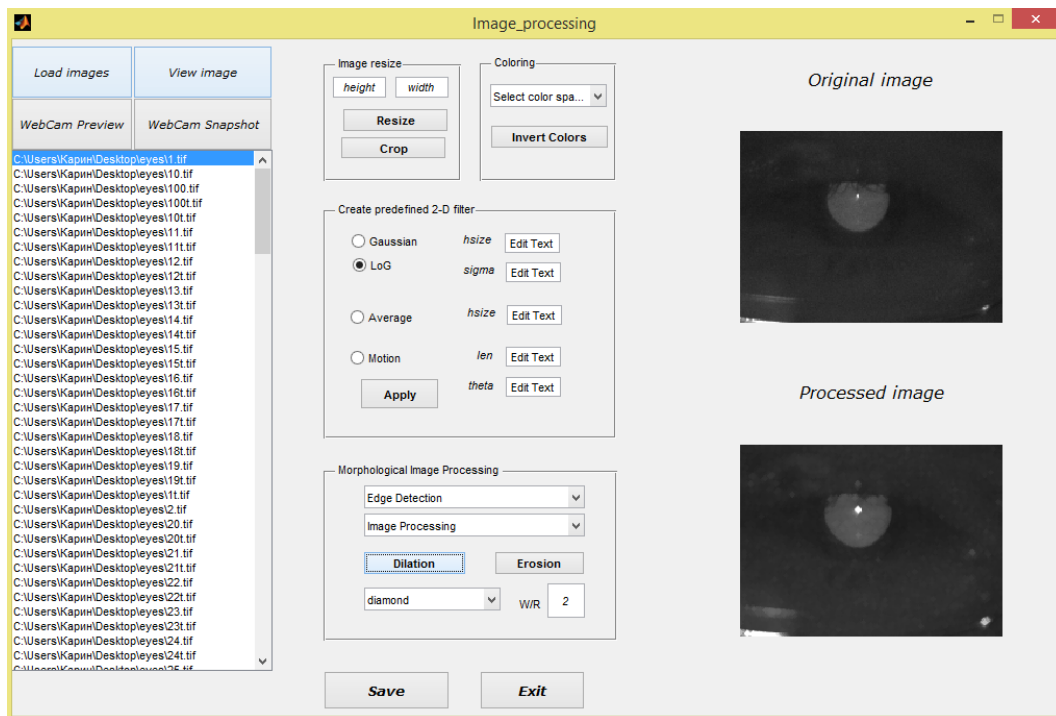


Figure 16 Interface of *Image\_processing* program

The following options are available in the program:

**uploading images.** There are 3 alternatives of loading images:

- from a text file containing a list of pictures;
- direct guidance of folder with images;
- take a picture of webcam.

**saving.** Possibility to save the processed image; the format and directory is selected by user.

**operations.** Among the possible processing operations are image resize, color map change, filtration, edge detection and other morphological image processing. More detailed description is provided in Appendix B. For creating the program were used MATLAB Documentation and [39].

## 5.2.2 Edge detectors comparison

### Methodology [40]

The experiment is done to compare five edge detection algorithms such as Sobel, Canny, Laplacian of Gaussian, Prewitt, and Roberts. The test images taken for analysis are the same as used in other experiments in this thesis. The test is based on the performance of operators with MSE<sup>1</sup> and PSNR<sup>2</sup>[40]. First, edge detection of test images is performed by applying all selected algorithms using Matlab software. The second stage is to calculate PSNR and  $MSE$  between each resultant edge detected image and ground truth image. The following equations were used for calculations:

$$PSNR = 10 \log_{10} \left( \frac{R^2}{MSE} \right), \quad (19)$$

where  $R$  is the maximal variation in the input image data. If it has an 8-bit unsigned integer data type,  $R$  is 255.

$$MSE = \frac{1}{M \times N} \sum_{M,N} [I_1(m, n) - I_2(m, n)]^2, \quad (20)$$

where,  $I_1$  is original image,  $I_2$  is edge detected image,  $m$  and  $n$  are height and width of the image respectively.

### Results and conclusion

All images were processed in the same manner for achieving the final results. The numeric results show <https://ru.sharelatex.com/project/553eb8305648356b5ad0af72wn> in table 3 and figures 17, 18 (all resultant tables and enlarged diagrams are also provided in Appendix A).

The PSNR metrics should be high in decibel for effective edge detected image. Sobel gives average ratio of 15.29 [dB] in contrast to Canny, which gives ratio of 15.309 [dB]. Expectedly, reversed situation with MSE is a minimal average ratio by Canny (1933.73) and maximal by Sobel (1941.897).

---

<sup>1</sup>Mean Squared Error. MSE incorporates degradation function and statistical characteristics of noise in the edge detected image. It measures the average squared difference between the estimator and the parameter. MSE specifies the average difference of the pixels throughout the original ground truth image with edge detected image.

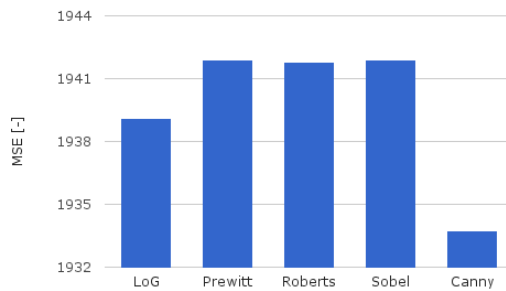
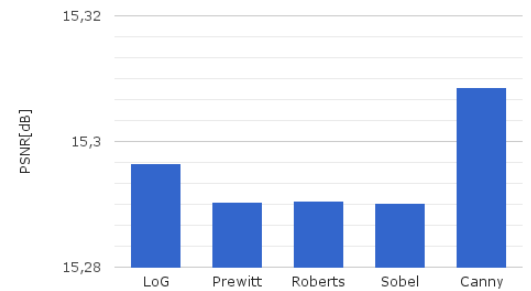
<sup>2</sup>Peak signal-to-noise ratio, is ratio between the maximum possible power of a signal and the power of corrupting noise that affects the fidelity of its representation.



When looking at processing time the best results are performed by Prewitt operator. Canny detector's time consumption is clearly inferior to Prewitt's one-it takes 8.35 times higher. The most significant factor contributing to this difference is that Canny uses two thresholds in contrast to the others.

**Table 3** Experimental edge detectors results

	LoG	Prewitt	Roberts	Sobel	Canny
Time [s]	0.0398	0.0083	0.0086	0.0106	0.0693
Average MSE [-]	1939.1003	1941.8726	1941.7632	1941.8974	1933.7310
Average PSNR [dB]	15.2965	15.2903	15.2905	15.2902	15.3086
Maximal MSE[-]	2251.4066	2253.7480	2253.4909	2253.7744	2246.3240
Maximal PSNR[dB]	15.7401	15.7333	15.7328	15.7333	15.7539

**Figure 17** Diagram of MSE results**Figure 18** Diagram of PSNR results

To conclude, on the basis of facts above, the better results were demonstrated by Canny edge detector in spite of high time consumption. It is optimal edge detection algorithm.

## 5.3 Daugman algorithm's improvement proposals

### 5.3.1 Reduction of processing area

By hypothesis, it is possible to minify the algorithms' computational time by reducing processing area of the image. This presumption was overthrown at a stage of theory studies due to the fact that resizing is already conducted in the code. Libor Mašek in

his thesis [37] states that iris images are first scaled to have constant diameter so that when comparing two images, one is considered as the reference image.

### 5.3.2 Improvements based on the usage of the data obtained from the previous frame

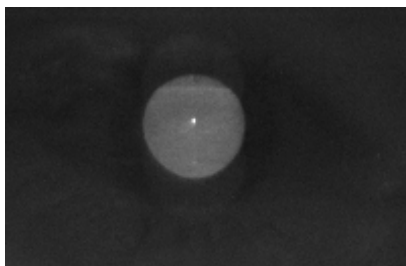
The difference between the two neighbouring images of video sequence is minimal, except in cases of eye movement (blinking). On this basis, the hypothesis of the possibility of accelerating the algorithm through data obtained from the previous image was put forward and verified. As it can be shown from data below, routine's time dropped at 4.88 times.

	original time	after modifications
execution time for 25 images	24,39	5,0
average algorithm's	0,98	0,2

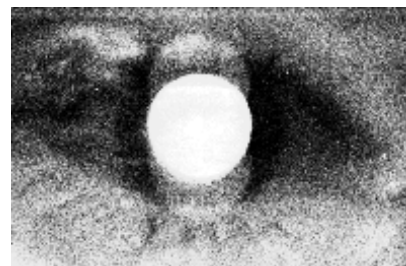
**Table 4** Algorithms' time consumption before and after proposed technique

### 5.3.3 Improvements based on the preliminary image preparation

The histogram equalization is supposed to be very effective in terms of image preprocessing, that's why it was tested primarily.



a) original image



b) after *histeq*

**Figure 19** Example of *histeq* application

	time [s]	radius accuracy
before	27.39067	98%
after	272,7848	94%

**Table 5** *histeq* experimental results

As it shown from the table 5, both the time consumption and the accuracy became worse.

The next step was to test different filters and morphological operations. By trial and error the following algorithm was chosen:

1. edge detecting;
2. dilation;
3. erosion;

First of all, the edge detector is applied to detect the pupil's edge (Prewitt operator was used due to its speed). The obtained image has openings, so white pixels are extended to close the image contour. For this purpose, the morphological operation *dilation* implemented in Matlab as functions' combination *strel* and *imdilate* is used. Next function *erode* is called to obviate the fact of superfluous line width. The resultant image contains the pupil's contour and minimal noise.

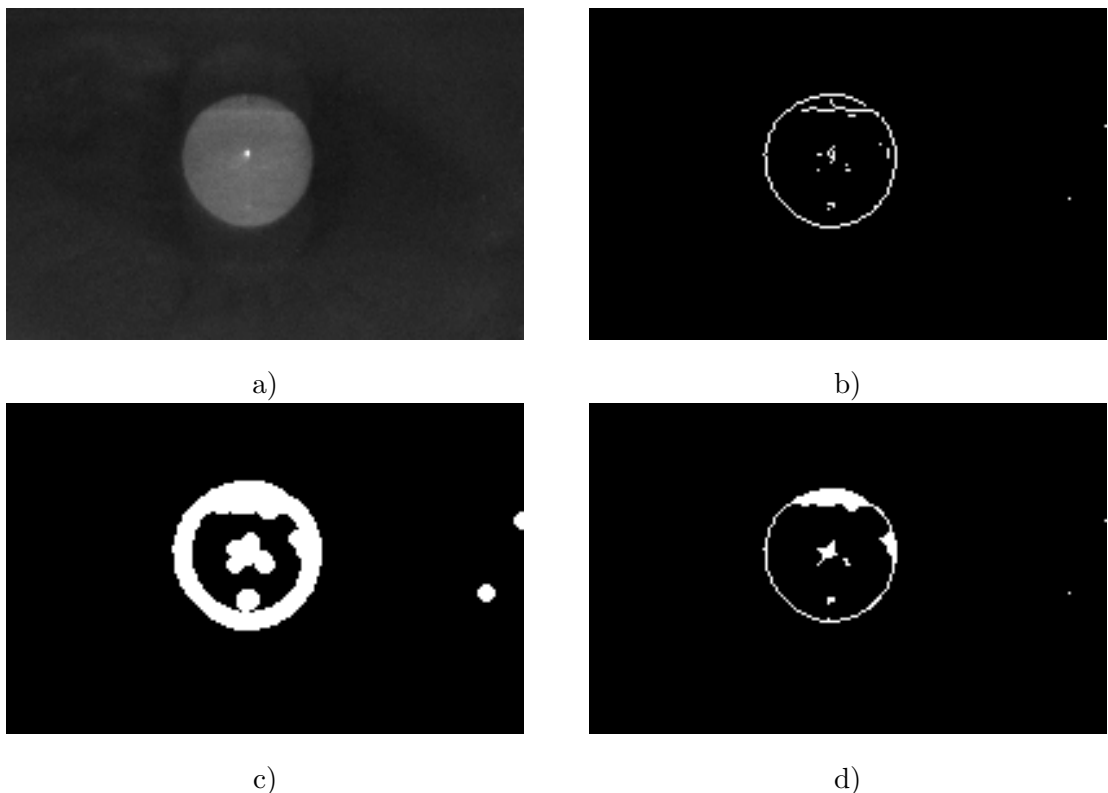


**Figure 20** Proposed algorithm: a) original image, b) detected edges, c) extension of white pixels, d) the previous image after *erosion*.

### 5.3.4 Adaboost technique

As an peculiar preprocessing method is possible to use method of simple classifiers strengthen called *Adaboost* followed by refinement of the inner iris boundary by Daugman algorithm. Strengthening the simple classifiers is an approach to solving the problem of classification, by combining some simple classifiers into one strong classifier.

By strength of the classifier in this case is understood the effectiveness of solving the problem of classification. A simple classifier is the following:

$$h(x, f, p, \Theta) = \begin{cases} 1, & pf(x) < p\Theta \\ 0, & otherwise \end{cases}, \quad (21)$$

where  $f$  is feature,  $p$  denotes polarity which indicates the direction of the irregularities,  $\Theta$  is a threshold value. The final strong classifier can be defined as:

$$C(x) = \begin{cases} 1, & \sum_{t=1}^{\tau} \alpha_t h_t(x) \geq \frac{1}{2} \sum_{t=1}^{\tau} \alpha_t \\ 0, & otherwise \end{cases}, \quad (22)$$

Figures below demonstrate result of Adaboost and Daugman methods combination. The full detailed description of this technique can be founded in [41]

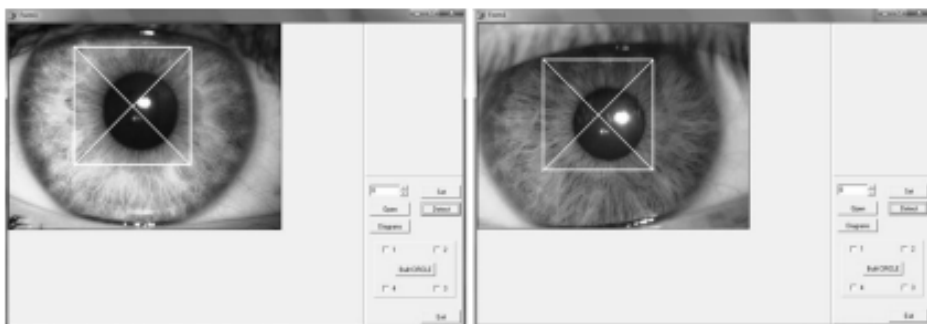


**Figure 21** Adaboost result. Image taken from [41]

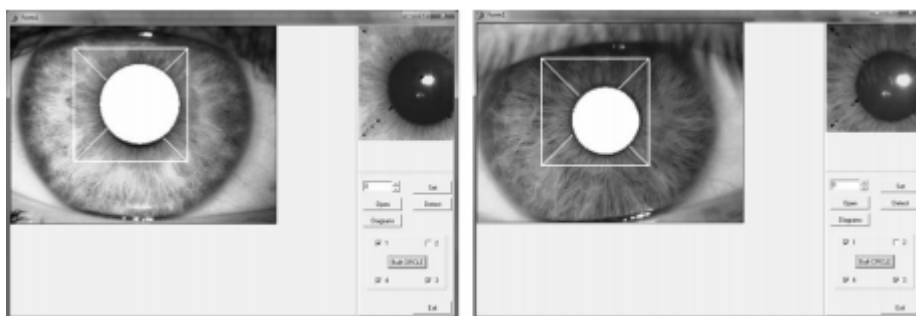


**Figure 22** Daugman algorithm was applied on figure 21. Image taken from [41]

## 6 Conclusion

The aim of this bachelor thesis is to familiarize with the problems of the analysis' parameters of the human pupil in video sequence, to implement and analyze the selected algorithms in Matlab environment, as well as to offer a suitable method of image preprocessing.

A detailed analysis of the problems is carried out, it is described why and how the detection of the pupil in images works in the theoretical part contained in Chapters 2-4. Chapter 5 deals with the experiments performed and their results.

At the initial stage of the experimental part of the thesis such algorithms as Daugman, Daugman with Gabor filter, Starburst and Hough transformation were tested. According to the test results the most accurate algorithm is Daugman algorithm using Gabor filter, which showed 99% of accuracy. However, due to the fact that processing took quite a lot of time, this method could not be considered optimal. Daugman without Gabor filter inferior in terms of the accuracy just one per cent, but at the same it takes half the time. Thus, this option of the algorithm is considered to be the best of the above mentioned. Starburst method has showed the worst results.

In the next experiment, I have identified the best edge detector. 5 detectors are tested, namely: Sobel, Prewitt, Canny, LoG and Roberts. PSNR and MSE indicators are chosen as parameters for comparison. Based on the results obtained, Canny detector is found the best.

Then I have created a simple program for image preprocessing. The program has the following obvious defects, which later will be eliminated:

- the list of files includes all files in the folder, not only images. It is necessary to impose restrictions only on the image format. Attempts to create such a filter at this stage are not successful;
- introduce the possibility to use the already processed image for further processing;
- check of the image type compatibility with the operation is not introduced for

## 6 Conclusion

each operation.

Daugman algorithm without Gabor filter is chosen as the best one on the results of previous tests as an algorithm for attempts to modify. The original images are processed by different methods of preprocessing, and the appropriate method of image preprocessing is selected on the basis of the results obtained. In terms of the tested sequence, the following algorithm can be used:

1. edge detecting;
2. dilation;
3. erosion.

It is also offered the possibility of improving the algorithm using the Adaboost technology, then attempts to implement and test this method will be made.

# Appendix A

## The results of tests

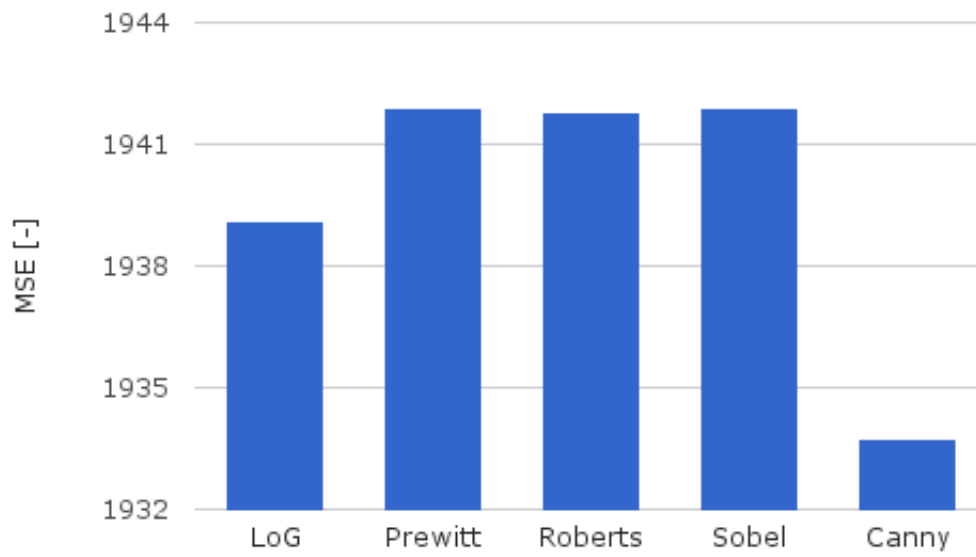
### A.1 Algorithms comparison

algorithm	Daugman	Daugman with Gabor	Starburst	Hough transformation
algorithm's execution time for 25 images [s]	24.391	50.661	25.896	0.955
average algorithm's execution time [s]	0.976	2.026	1.036	0.038
accuracy [%]	98	99	78	97
average precision center [pixels]	0.721	0.649	5.616	0.9296

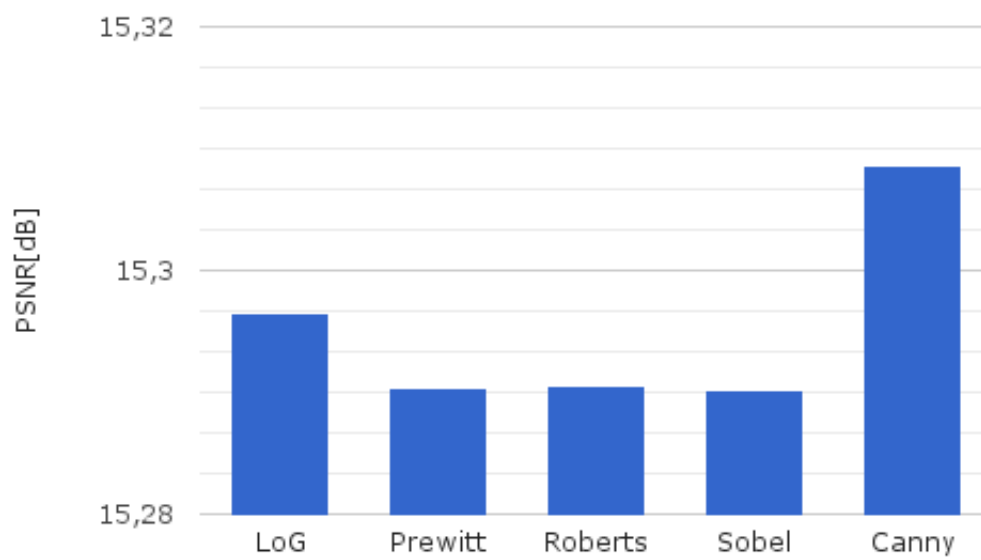
### A.2 Edge detectors comparison table

	LoG	Prewitt	Roberts	Sobel	Canny
Time [s]	0.0398	0.0086	0.0083	0.0106	0.0693
Average MSE [-]	1939.1003	1941.8726	1941.7632	1941.8974	1933.7310
Average PSNR [dB]	15.2965	15.2903	15.2905	15.2902	15.3086
Maximal MSE[-]	2251.4066	2253.7480	2253.4909	2253.7744	2246.3240
Maximal PSNR[dB]	15.7401	15.7333	15.7328	15.7333	15.7539

### A.3 MSE diagram



#### A.4 PSNR diagram



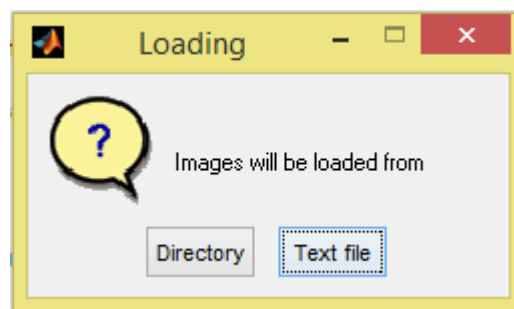


## Appendix B

### UserGuide of GUI Image\_processing

This program is a tool for image processing. It was created in Matlab environment and has a user-friendly graphical interface.

To upload images press the button *Load images* in the upper left corner. The following dialog window appears:



A *textfile* option requires a text document called images.txt to be located in the same folder as GUI is. It is possible to change a file name and location by changing the corresponding code lines. This file should contain the full name of the file path. If this is true, your images will be loaded to the list.

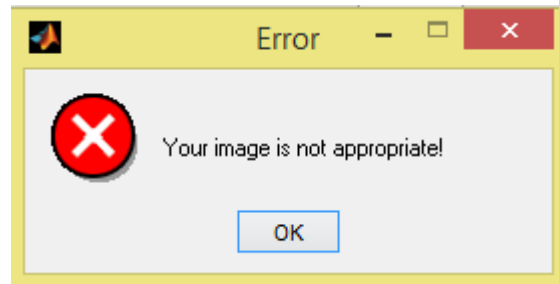
It is also possible to make a photo from webcam by clicking the *Webcam snapshot* button.

To preview selected images from the list, press the button *View image*. After that your images appear in the upper right corner of the workplace. For demonstrating original and processed images there are two windows labeled respectively to its purpose.

To resize your image enter desired height and width values into corresponding text boxes and click on the *Resize* button. A *crop* option creates a moveable, resizable rectangle that can be positioned interactively. Using the mouse you can specify the crop rectangle by clicking and dragging the mouse. When you finish sizing and positioning

the crop rectangle, create the cropped image by double-clicking the left mouse button.

The panel *Coloring* has two options: to change the image color map or simply invert colors in the image. If your image has an inappropriate type, you will see this warning box:



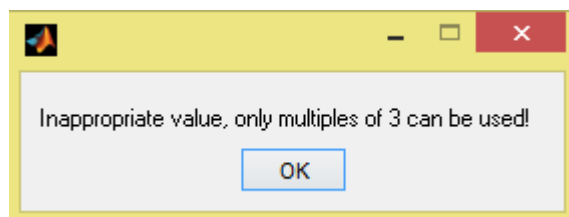
The panel *Create predefined 2-D filter* makes it possible to filtrate your image by means of the LoG, Gaussian, Average, and Motion filters. Choose the filter, enter required parameters and press the button *Apply*.

The panel *Morphological Image processing* has three options:

- Edge detection (Canny, Sobel, Prewitt, Roberts, LoG operators are proposed)
- Morphological operations on binary images (bwmorph)
- Erosion/Dilation

Pop-up menus open to display a list of options when you click the arrow.

To dilate or erode your image using the structuring element SE and its value should be preliminary specified. It is necessary to note that values of octagon and square strels can be only multiplied by 3. Otherwise you will see:



To save the processed image click on the button *Save*, to exit click on the *Exit* button.

# Appendix C

## CD content

- \images – original graphic files;
- \source\_codes – algorithms' implementation in Matlab;
- \imageGUI – ready-to-use image processing program;
- \results – obtained results as *.xlsx* tables;
- \thesis – the thesis in PDF format

## Bibliography

- [1] A. Degtjareva and V. Vezhnevec. *Metody identifikacija lichnosti po raduzhnoj obolochke glaza*. In Russian. URL: <http://www.cgm.computergraphics.ru/content/view/61> (visited on 20/05/2015).
- [2] “Eye tracking”. In: *Wikipedia: the free encyclopedia* (2001-2015). URL: [http://en.wikipedia.org/wiki/Eye\\_tracking](http://en.wikipedia.org/wiki/Eye_tracking) (visited on 20/05/2015). San Francisco (CA): Wikimedia Foundation.
- [3] V.A. Barabanschikov. *Okulomotornye struktury vospriyatiya*. in Russian. 1997. ISBN: 5-02-13318-3. URL: <http://zreni.ru/1601-metody-okulografii-v-issledovanii-poznavatelnyh-processov-i-deyatelnosti.html> (visited on 20/05/2015).
- [4] Image by T. Winslow. *Intraocular Melanoma Of The Iris*. URL: <http://www.harvard-wm.org/the-body-of-human-eyes/intraocular-melanoma-of-the-iris/> (visited on 20/05/2015).
- [5] “Gaussian\_function”. In: *Wikipedia: the free encyclopedia* (2001-2015). URL: [http://en.wikipedia.org/wiki/Gaussian\\_function#/media/File:Gaussian\\_2d.svg](http://en.wikipedia.org/wiki/Gaussian_function#/media/File:Gaussian_2d.svg) (visited on 20/05/2015). San Francisco (CA): Wikimedia Foundation.
- [6] V.I. Bobrova and S.N. Nikiforov. “Znachenie izmenenij zrachkov v diagnostike nevrologicheskikh zabolevanij”. in Russian. In: *Medicina neotlozhnykh sostojanij* 4(5) (2006). URL: <http://www.mif-ua.com/archive/article/1070>.
- [7] M. Green. *Night Vision*. URL: <http://www.visualexpert.com/Resources/nightvision.html> (visited on 20/05/2015).
- [8] M. Millodot. *Dictionary of optometry and visual science*. 7th ed. New York: Elsevier/Butterworth-Heinemann, 2009. ISBN: 07-020-2958-0. URL: <http://medical-dictionary.thefreedictionary.com/Purkinje+shift> (visited on 20/05/2015).

- [9] *Purkinje Effect*. Grand Illusions Ltd. URL: [http://www.grand-illusions.com/articles/purkinje\\_effect/](http://www.grand-illusions.com/articles/purkinje_effect/) (visited on 20/05/2015).
- [10] URL: [http://pixabay.com/p-165916/?no\\_redirect](http://pixabay.com/p-165916/?no_redirect) (visited on 20/05/2015).
- [11] URL: <http://isle.hanover.edu/Ch03Eye/Ch03PurkinjeSim.html> (visited on 20/05/2015).
- [12] “Purkinje images”. In: *Wikipedia: the free encyclopedia* (2001-2015). URL: [http://en.wikipedia.org/wiki/Purkinje\\_images](http://en.wikipedia.org/wiki/Purkinje_images) (visited on 20/05/2015). San Francisco (CA): Wikimedia Foundation.
- [13] J. Dušek and T. Jindra. “Measuring Biomechanics of the Vision Process, Sensory Fusion and Image Observation Features”. In: *Technologies for Medical Sciences*. Springer, 2012. London.
- [14] K. Chen and H.J. Choi. *Visual Attention and Eye Movements*. URL: <http://www.ics.uci.edu/~majumder/vispercep/paper08/visualattention.pdf> (visited on 20/05/2015).
- [15] URL: <http://www.eyecalcs.com/DWAN/pages/v1/ch002/006f.html> (visited on 20/05/2015).
- [16] “Vergence”. In: *Wikipedia: the free encyclopedia* (2001-2015). URL: <http://en.wikipedia.org/wiki/Vergence> (visited on 20/05/2015). San Francisco (CA): Wikimedia Foundation.
- [17] “Vestibulo–ocular reflex”. In: *Wikipedia: the free encyclopedia* (2001-2015). [http://en.wikipedia.org/wiki/Vestibulo\\_ocular\\_reflex](http://en.wikipedia.org/wiki/Vestibulo_ocular_reflex)(visited on 20/05/2015). San Francisco (CA): Wikimedia Foundation.
- [18] “Optokinetic reflex”. In: *Wikipedia: the free encyclopedia* (2001-2015). URL: [http://en.wikipedia.org/wiki/Optokinetic\\_reflex](http://en.wikipedia.org/wiki/Optokinetic_reflex) (visited on 20/05/2015). San Francisco (CA): Wikimedia Foundation.
- [19] URL: [https://beingspecialdotorg.files.wordpress.com/2013/02/neurology\\_of\\_nystagmus\\_1.jpg](https://beingspecialdotorg.files.wordpress.com/2013/02/neurology_of_nystagmus_1.jpg) (visited on 20/05/2015).
- [20] “Computerized Pupillometry: From a Research Tool to Clinical Diagnostics”. In: (Mar. 2005). Ed. by Ph.D. Murat V. Kalayoglu M.D. URL: <http://www.opthalmologyweb.com/Tech-Spotlights/26437-Computerized-Pupillometry-From-a-Research-Tool-to-Clinical-Diagnostics/> (visited on 20/05/2015).

## Bibliography

- [21] “Edge detection”. In: *Wikipedia: the free encyclopedia* (2001-2015). URL: <http://en.wikipedia.org/wiki?curid=331680> (visited on 20/05/2015). San Francisco (CA): Wikimedia Foundation.
- [22] Trucco and Jain et al. *Edge Detection*. Chapter 4 and chapter 5. URL: <http://www.cse.unr.edu/~bebis/CS791E/Notes/EdgeDetection.pdf> (visited on 20/05/2015).
- [23] S. Saluja, A.K. Singh, and S. Agrawal. *A Study of Edge-Detection Methods*. URL: <http://www.ijarcce.com/upload/january/20-A%20Study%20of%20Edge-Detection.pdf> (visited on 20/05/2015).
- [24] P.K. Kalra. *Canny Edge Detection*. URL: <http://www.cse.iitd.ernet.in/~pkalra/csl783/canny.pdf> (visited on 20/05/2015).
- [25] Masoud Nosrati et al. “Edge Detection Techniques in Processing Digital Images: Investigation of Canny Algorithm and Gabor Method”. In: *World Applied Programming* 3.3 (2013), pp. 116–121.
- [26] *Gaussian Smoothing*. School of Informatics, The University of Edinburgh. URL: <http://homepages.inf.ed.ac.uk/rbf/HIPR2/gsmooth.htm> (visited on 20/05/2015).
- [27] R. Donida Labati et al. *Iris segmentation: state of the art and innovative methods*. URL: <http://piurilabs.di.unimi.it/Papers/Iris%20segmentation%20state%20of%20the%20art%20and%20innovative%20methods.pdf> (visited on 20/05/2015).
- [28] “Gabor filter”. In: *Wikipedia: the free encyclopedia* (2001-2015). URL: [http://en.wikipedia.org/wiki/Talk:Gabor\\_filter](http://en.wikipedia.org/wiki/Talk:Gabor_filter). San Francisco (CA): Wikimedia Foundation.
- [29] P. Moreno, Re Bernardino, and J. Santos-Victor. “Gabor parameter selection for local feature detection”. In: *in Proc. of the 2nd IBPRIA*. 2005.
- [30] T. Jindra and S. Vitek. “Analysis of brightness profiles during eccentric photorefraction – comparison of pupil localization algorithms”. in Czech. In: *21th Annual Conference Proceedings Technical Computing Prague 2013*. HUMUSOFT, 2013.
- [31] J. Daugman. “How Iris Recognition Works”. Invited Paper. ISBN: 10.1109/tcsvt.2003.818350. URL: <http://www.cl.cam.ac.uk/~jgd1000/csvt.pdf> (visited on 20/05/2015).

- [32] O. Percy and A. Waqas. “Iris localization using Daugman’s algorithm”. bachelor’s thesis. Blekinge Institute of Technology. URL: [http://www.bth.se/fou/cuppsats.nsf/a11/547cf4484a703e90c1257990000c5d3c/%5C\\$file/BTH20110ad.pdf](http://www.bth.se/fou/cuppsats.nsf/a11/547cf4484a703e90c1257990000c5d3c/%5C$file/BTH20110ad.pdf) (visited on 20/05/2015).
- [33] K. Marinichev and V. Vezhnevcev. *Algoritmy vydeleniya parametriceskix krivyx na osnove preobrazovanie Xafa*. In Russian. URL: <http://cgm.computergraphics.ru/content/view/107> (visited on 20/05/2015).
- [34] MATLAB Documentation. *Imfindcircles: Find circles using circular Hough transform*. URL: <http://www.mathworks.com/help/images/ref/imfindcircles.html> (visited on 20/05/2015).
- [35] D. Li and D.J. Parkhurst. “Starburst: A robust algorithm for video-based eye tracking”. Elsevier Science.
- [36] T.Prat and S. Vítek. “Advanced Image Processing : pupil detection of the eyes”. Internship report. Czech Technical University, 2013.
- [37] L. Mašek. “Recognition of Human Iris Patterns for Biometric Identification”. Technical report. The University of Western Australia, 2003.
- [38] MATLAB Documentation. *Imcomplement: Complement image*. URL: <http://www.mathworks.com/help/images/ref/imcomplement.html> (visited on 20/05/2015).
- [39] V.P. D’jakonov. *MATLAB i SIMULINK dlja radioinzhenerov*. In Russian. DMK izdatel’stvo, 2013. ISBN: 978-5-94074-897-7. Moscow.
- [40] D. Poobathy and R. Manicka Chezian. *Edge Detection Operators: Peak Signal to Noise Ratio Based Comparison*. URL: <http://www.mecs-press.org/ijigsp/ijigsp-v6-n10/IJIGSP-V6-N10-7.pdf> (visited on 20/05/2015).
- [41] N. V. Voloshin. *Metod opredelenija zrachka v avtomaticheskix sistemah iridodiagnostiki*. In Russian and Ukrainian. URL: <http://www.kpi.kharkov.ua/archive/> (visited on 20/05/2015).